

1

1,2 2 . 2 . 2 . 2

: 가
 : 3.0 T 32 30 (10 -
 90 , 43) . ,
 11 638 . 28
 (8 , 20), 34 (22 , 12).
 가 (maximal
 relative enhancement (MRE), time to peak (TTP), wash in rate (WI)
 (SS))
 : TTP, WI, , SS
 ($p < 0.05$), MRE . TIC

(MRI) first-pass data
 가 가 , ,
 가
 (1-3). , Crim (3) MRI가
 (maximal relative enhancement,
 MRE), time to peak (TTP), wash in rate (WI), steepest
 slope (SS), , first pass TIC 가
 (region of
 interest, ROI) - (time intensity curve,
 TIC)
 가가 가 . Erlemann (6) 가
 80% 가
 Ewing

(5).

1994 Verstraete (7)

가

62 (30, 32; 10-90 ,

43)

28

(8 ,

2007 8 16

2007 12 26

20), 34 (22 , mmol/kg body weight) (SPECTRIS; MEDRAD, Pittsburgh, U.S.A.)
 12). 가 T1

MR
 MR 3.0 T (Achieva 3.0T X - series; Version release 2.0, Philips, Netherlands) system
 MRI series(spin - echo T1, T2, T2 MRE, WI, TTP (software system) 가
 , T1 ((sequence)) 가
 (58 short T1 - weighted fast field - echo (FFE) 가
 (TR/TE=7.4/3.9, flip angle=25 °, field of view=200 - 250 mm; section thickness=5 mm without intersection gap in every 5 seconds)). 320
 11 638
 12 gauge
 3 mL a bolus of gadopentate dimeglumine(DOTA; Schering, Berlin, Germany; 0.1

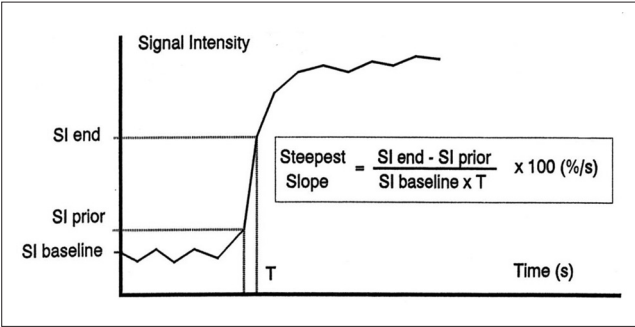


Fig. 1. In a time-intensity curve, the temporal change of the signal intensity in a region of interest (ROI) is plotted against time. The steepest slope represents the highest enhancement during first pass and is mainly determined by tissue vascularization and perfusion.

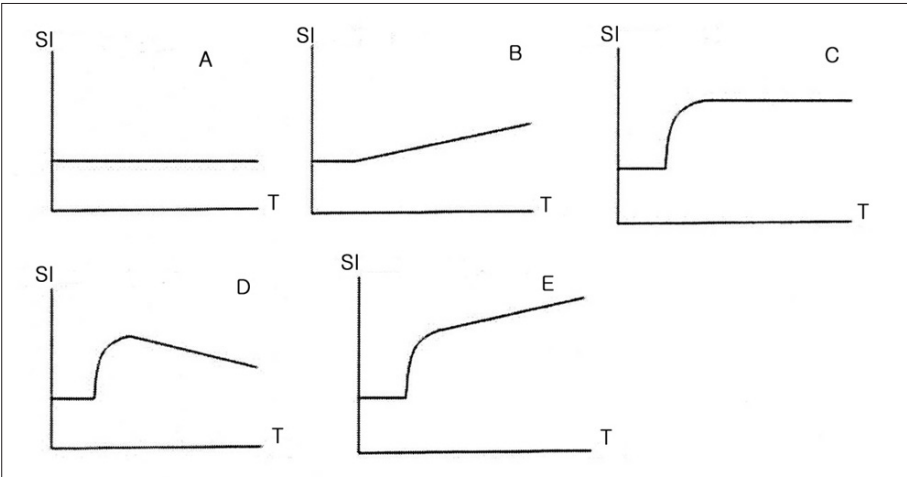


Fig. 2. Five types of time intensity curve plotted from a dynamic perfusion MR imaging of the musculoskeletal lesions. (SI: signal intensity, T: time)

Software system(Philips)
 (Fig. 1). TIC (SIbase) TIC (SImax) 가
 Slend (T) Slprior Slend 가
 MRE, WI, TTP software system ()
 SS Buadu (8) (SS = ((Slend - Slprior)/SIbase x T)) x 100 (%/sec)). nonparametric test
 ROC Osamu (9) (Fig. 2), Type A , Type B 가 , Type C 가

(wash - in) (plateau) (wash - in)
 , Type D (wash - out phase)
 Type E

type A B
 , type C - E

, TIC

(n = 30)

(n = 32)

Table 1

MRE, TTP, WI, SS

Table 2 . Levene test

가

(nonparametric Mann - Whitney

test))

TTP ($p = 0.0008$), WI ($p = 0.0023$), SS

($p = 0.0017$)

가 , MRE

ROC

MRE

SS

ROC

가

(Table 3, Fig. 3).

7.4

SS

97%, 57%, 70%,

94%,

77%

,

26

, WI

91%,

57%, 69%, 85%,

74%

224

Table 1. Benign and Malignant Lesions

Malignant Lesions (n = 32)	
metastasis	(n = 8),
osteosarcoma	(n = 5),
extraskeletal sarcomas	(n = 4),
lymphoma	(n = 4),
malignant fibrous histiocytoma	(n = 4),
dermatofibrosarcoma protuberans	(n = 2),
multiple myeloma	(n = 2),
chondrosarcoma	(n = 1),
hemangiopericytoma	(n = 1),
melanoma	(n = 1).
Benign Lesions (n = 30)	
neurogenic tumor	(n = 8),
hemangioma	(n = 4),
chronic inflammation	(n = 2),
fibromatosis	(n = 2),
lipoma	(n = 2),
stress fracture	(n = 2),
simple bone cyst	(n = 1),
fibrous dysplasia	(n = 1),
giant cell tumor	(n = 1),
epidermal cyst	(n = 1),
ganglion cyst	(n = 1),
glomus tumor	(n = 1),
intraosseous lipoma	(n = 1),
enchondroma	(n = 1),
marrow reconversion	(n = 1),
cavernous malformation	(n = 1).

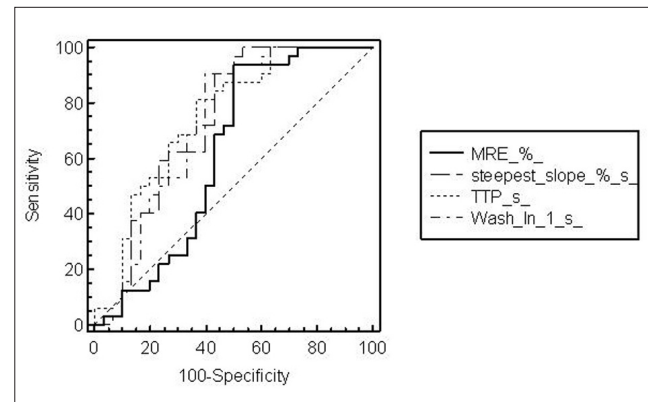


Fig. 3. Results of ROC curve Analysis for four parameters

Table 2 Range of Values and Mean Values of Perfusion Parameters

Parameter	Benign		Malignant		P-value
	Range	Mean	Range	Mean	
MRE (%)	3.9 - 764.1	229.56	98.4 - 725.1	272.5	0.1115
TTP (s)	15.2 - 307.2	195.3	10.3 - 258.3	107.4	0.0008
WI (1/s)	4.1 - 365.7	64.7	7.4 - 334.1	82.6	0.0023
SS (%/s)	0.09 - 78.99	12.6	2.75 - 70.92	18.9	0.0017

Note. MRE: maximal relative enhancement, TTP: time to peak, WI: wash in rate, SS: steepest slope

Table 3. Results of ROC Curve Analysis for Four Parameters

Parameter	Area under the ROC	Criterion	Sensitivity	Specificity	+ LR	- LR
MRE	0.618	> 148.4	93.7	50.0	1.87	0.13
TTP	0.748	< 224.5	78.1	63.3	2.22	0.30
WI	0.725	> 23.7	90.6	57.0	2.27	0.16
SS	0.732	> 7.39	97.0	56.7	2.09	0.17

TTP 78%, 63%, 69%, 73%, 71%

TIC

Fisher's exact test (Table 4).

A B

= 0.007 and 0.027)(Fig. 4), D

($p = 0.0079$) (Fig. 5).

C E

($p > 0.05$). TIC

Table 4. Distribution of the Five Types of Time-intensity Curves in Benign and Malignant Musculoskeletal Lesions

Curve pattern	Benign	Malignant	Total	P-value
A	6	0	6	0.010
B	10	1	11	0.002
C	4	9	13	0.215
D	5	17	22	0.004
E	5	5	10	1
Total	30	32	62	

Note. p -values are calculated by Fisher's exact test.

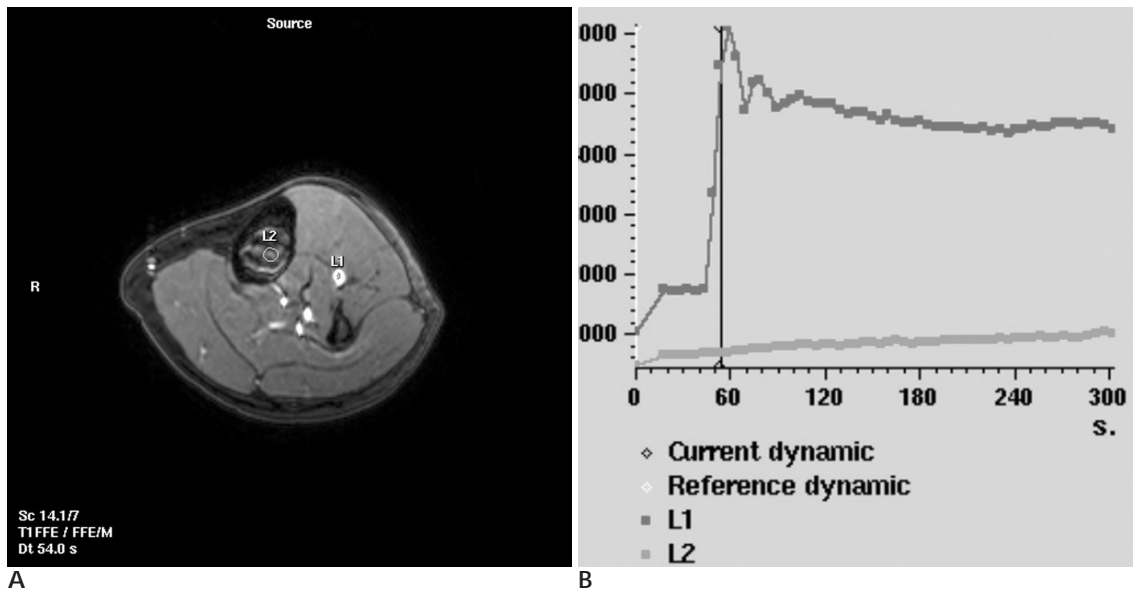


Fig. 4. A 52 year-old woman with histologically proved enchondroma of the tibial shaft. (A) Postcontrast T1-FFE sequences shows heterogeneously mild enhancement of the lesion. (B) Time intensity curve demonstrates a slowly inclined curve (Type B).

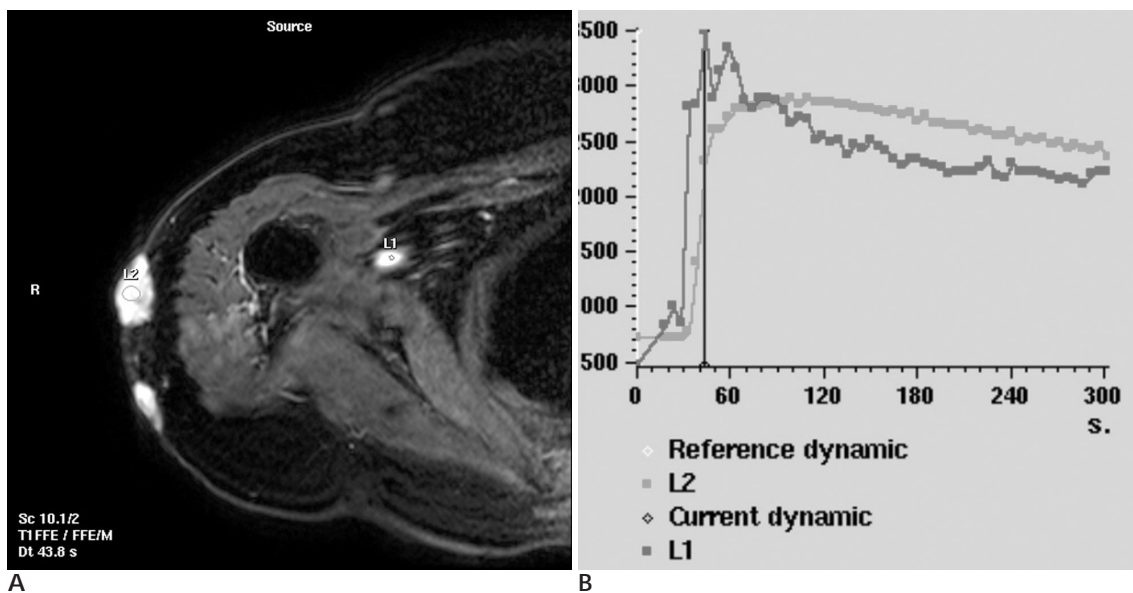


Fig. 5. A 68 year-old woman with histologically proved dermatofibrosarcoma protuberans involving right shoulder. (A) Postcontrast T1-FFE sequences shows homogeneously hyperenhancing mass. (B) Time intensity curve demonstrates a rapidly rising slope (wash-in) during an initial short period, followed by a wash-out phase (Type D).

97%, 53%, 69%, 94%, 76%

(2, 7, 10).

가 , (5-7, 9-18). 가 MRI (Ultra fast MRI sequence) 가 ,

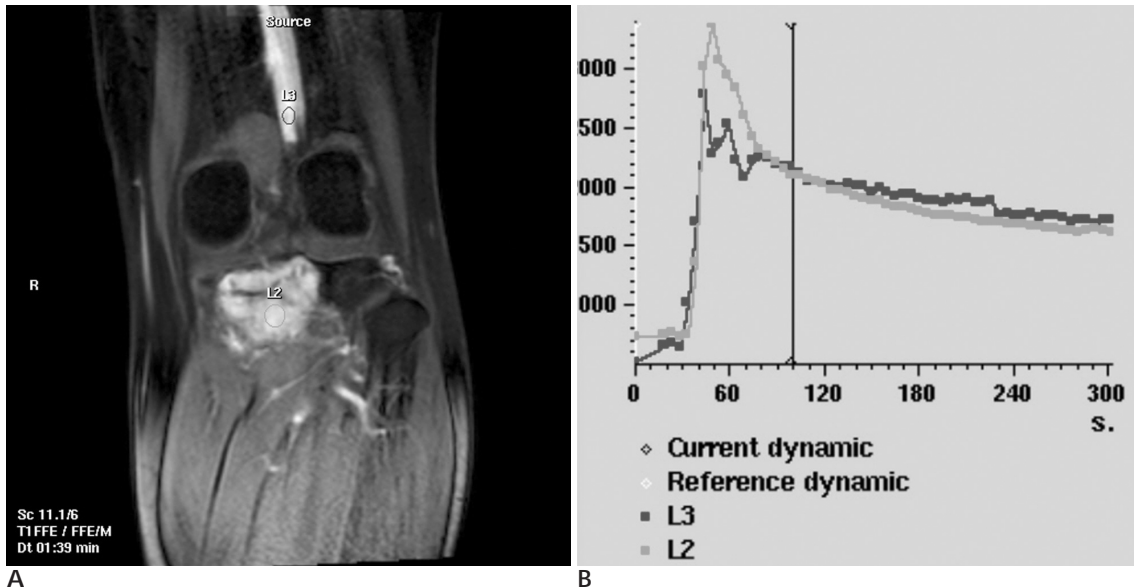


Fig. 6. A 22 year-old woman with histologically proved giant cell tumor of the proximal tibia. (A) Postcontrast T1-FFE sequences shows strong enhancement of the lesion. (B) The lesion is benign, but, time intensity curve demonstrates a rapidly rising slope (wash-in) during an initial short period, followed by a wash-out phase (Type D).

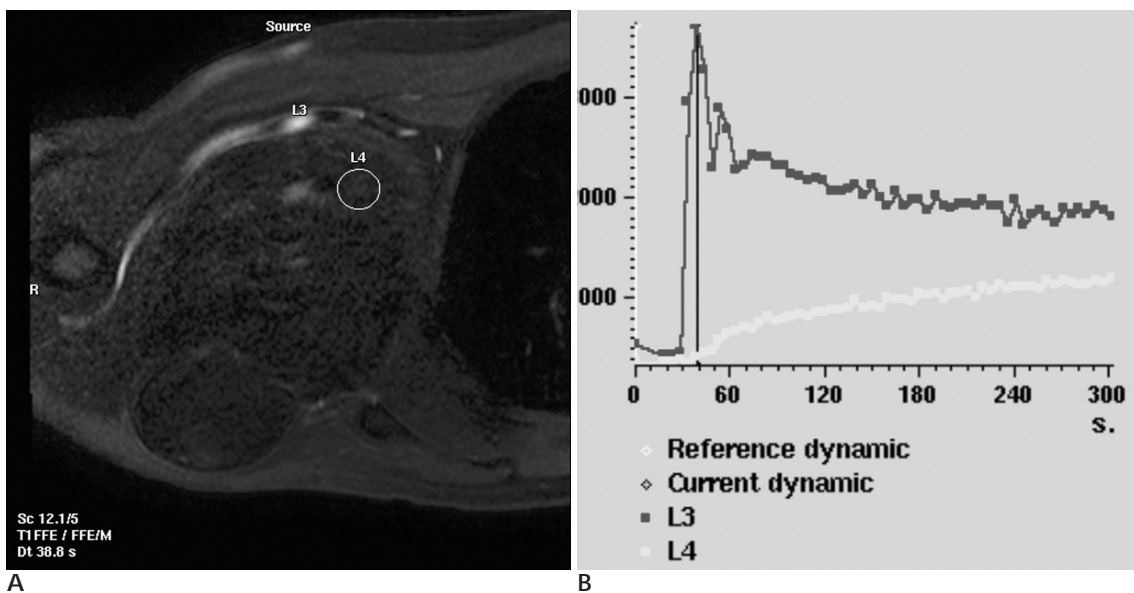


Fig. 7. A 35 year-old man with histologically proved extraskeletal chondrosarcoma in right axilla. (A) Postcontrast T1-FFE sequences shows poor enhancement of the lesion. (B) The lesion is malignant, but, time intensity curve demonstrates slowly gradual enhancement (Type B).

,

(22).

가

가

. Vanel (23, 24)

가

가

가

(2, 7, 10).

가

(19 - 21).

TIC

SS

TTP, WI, , SS

(

)

가 (Fig. 6),

(Fig. 6),

가

(

(Fig. 7).

Type B TIC

TIC

•

SS

91 - 72%

가

color map

가

가.

TIC

가

TIC

, A B

, D

C D

TIC

가

1. Aisen AM, Märtel W, Braunstein EM, McMillin KI, Phillips WA, Kling TF. MRI and CT evaluation of primary bone and soft tissue tumors. *AJR Am J Roentgenol* 1986;146:749-56
2. Hough TJ, Tung GA, Terek RM. *Staging, characterization, and grading*. In De Schepper AM, Vanhoenacker F, Gielen J, Parizel PM. *Imaging of soft tissue tumors*. 3rd ed. Berlin: Springer; 1997;113-25
3. Crim JR, Seeger LL, Yao L, Chandnani V, Eckardt JJ. Diagnosis of soft-tissue masses with MR imaging: can benign masses be differentiated from malignant ones? *Radiology* 1992;185:581-586
4. Kransdorf MJ, Murphey MD. *Imaging of soft tissue tumors*. Philadelphia: W.B. Saunders; 1997
5. Erlemann R, Reiser MF, Peters PE, Vasallo P, Nommensen B, Kusnierz-Glaz CR, et al. Musculoskeletal neoplasm: static and dynamic Gd-DTPA-enhanced MR imaging. *Radiology* 1989;171:767-773
6. Erlemann R, Sciuk J, Bosse A, Ritter J, Kusnierz-Glaz CR, Peters PE, et al. Response of osteosarcoma and Ewing sarcoma to preoperative chemotherapy assessment with dynamic and static MR imaging and skeletal scintigraphy. *Radiology* 1990;175:791-796
7. Verstraete KL, De Deene Y, Roels H, Dierick A, Uyttendaele D, Kunnen M. Benign and malignant musculoskeletal lesion: dynamic contrast-enhanced MR imaging-parametric "first-pass" images depict tissue vascularization and perfusion. *Radiology* 1994;192:835-843
8. Buadu LD, Murakami J, Murayama S, Hashiguchi N, Sakai S, Masuda K, et al. Breast lesions: correlation of contrast medium enhancement patterns on MR images with histopathologic findings and tumor angiogenesis. *Radiology* 1996;200:639-649
9. Tokuda O, Hayashi N, Taguchik K, Matsunaga N. Dynamic contrast-enhanced perfusion MR imaging of diseased vertebrae: analy-

- sis of three parameters and the distribution of the time-intensity curve patterns. *Skeletal Radiol* 2005;34:632-638
10. Ma LD, Frassica FJ, McCarthy EF, Bluemke DA, Zerhouni EA. Benign and malignant musculoskeletal masses: MR imaging differentiation with rim-to-center differential enhancement ratios. *Radiology* 1997;202:739-44
 11. Fletcher BD, Hanna SL, Fairclough DL, Gronemeyer SA. Pediatric musculoskeletal tumors: use of dynamic contrast-enhanced MR imaging to monitor response to chemotherapy. *Radiology* 1992;184:243-248
 12. Mirowitz SA, Totty WG, Lee JK. Characterization of musculoskeletal masses using dynamic Gd-DTPA enhanced spin-echo MRI. *J Comput Assist Tomogr* 1992;16:120-125
 13. Bollow M, Braun J, Hamm B, Eggens U, Schilling A, Konig H, et al. Early sacroiliitis in patients with spondylarthropathy: evaluation with dynamic gadolinium-enhanced MR imaging. *Radiology* 1995;194:529-536
 14. Reiser MF, Bongartz GP, Erlemann R, Schneider M, Pauly T, Sitteck P, et al. Gadolinium-DTPA in rheumatoid arthritis and related diseases: first results with dynamic magnetic resonance imaging. *Skeletal Radiol* 1989;18:591-597
 15. van der Woude HJ, Bloem JL, Verstraete KL, Taminiau AH, Nooy MA, Hogendoorn PC. Osteosarcoma and Ewing's sarcoma after neoadjuvant chemotherapy: value of dynamic MR imaging in detecting viable tumor before surgery. *AJR Am J Roentgenol* 1995;165:593-598
 16. Tuncbilek N, Karakas HM, Okten OO. Dynamic contrast enhanced MRI in the differential diagnosis of soft tissue tumors. *Eur J Radiol* 2005;53:500-505
 17. Verstraete KL, van der Woude HJ, Hogendoorn PC, De-Deene Y, Kunnen M, Bloem JL. Dynamic contrast-enhanced MR imaging of musculoskeletal tumors: basic principles and clinical applications. *J Magn Reson Imaging* 1996;6:311-321
 18. Hawighorst H, Libicher M, Knopp MV, Moehler T, Kauffmann GW, Kaick G. Evaluation of angiogenesis and perfusion of bone marrow lesions: role of semiquantitative and quantitative dynamic MRI. *J Magn Reson Imaging* 1999;10:286-294
 19. Preziosi P, Orlacchio A, Di Giambattista G, Di Renzi P, Bortolotti L, Fabiano A, et al. Enhancement patterns of prostate cancer in dynamic MRI. *Eur Radiol* 2003;13:925-930
 20. Liney GP, Gibbs P, Hayes C, Leach MO, Turnbull LW. Dynamic contrast-enhanced MRI in the differentiation of breast tumors: user-defined versus semi-automated region-of-interest analysis. *J Magn Reson Imaging* 1999;10:945-949
 21. Schaefer JF, Vollmar J, Schick F, Vonthein R, Vonthein R, Seemann MD, et al. Solitary pulmonary nodules: dynamic contrast-enhanced MR Imaging-perfusion differences in malignant and benign lesions. *Radiology* 2004;232:544-553
 22. van der Woude HJ, Bloem JL, Hogendoorn PC. Preoperative evaluation and monitoring chemotherapy in patients with high-grade osteogenic and Ewing's sarcoma: review of current imaging modalities. *Skeletal Radiol* 1998;27:57-71
 23. Vanel D, Shapeero LG, De Baere T, Gilles R, Tardivon A, Genin J, et al. MR imaging in the follow-up of malignant and aggressive soft tissue tumors: results of 511 examinations. *Radiology* 1994;190:263-268
 24. Vanel D, Tardivon A, Shapeero L, Western A, De Baere T, Guinebreiere JM. Dynamic contrast-enhanced subtraction MR imaging in follow-up of aggressive soft-tissue tumors: a prospective study of 74 patients (abstract). *Radiology* 1993;189(suppl):205

Diagnostic Value of Dynamic Perfusion MR Imaging in Benign and Malignant Musculoskeletal Lesions¹

Byeong Kyoo Choi, M.D.^{1,2}, Sang Hoon Lee, M.D., Ji Hyeon Cha, M.D., Sung Moon Kim, M.D.,
Myung Jin Shin, M.D., Heon Han, M.D.², Sam Soo Kim, M.D.²,
Ji Yeon Lee, M.D.², Yong Hwan Jeon, M.D.²

¹Department of Radiology, Asan Medical Center, University of Ulsan College of Medicine, Korea

²Department of Radiology, Kangwon National University College of Medicine, Korea

Purpose: To assess the diagnostic value of dynamic perfusion MR imaging for differentiation between benign and malignant musculoskeletal lesions.

Materials and Methods: Dynamic perfusion MR imaging was performed using a 3.0 T system in 32 female and 30 male patients (aged 10 - 90 years, mean age, 43 years). Following the assessment of the precontrast imaging, a dynamic study was performed. This dynamic technique allowed for 638 images to be obtained at 11 levels throughout the lesion. Twenty-eight lesions originated within bone (8 benign, 20 malignant), whereas 34 lesions were of soft tissue origin (22 benign, 12 malignant). The final diagnosis was histopathologically confirmed in all patients. To differentiate between benign and malignant lesions, we analyzed the four parameters: (maximal relative enhancement (MRE), time to peak (TTP), wash in rate (WI), steepest slope (SS) and the distribution of time intensity curve (TIC) patterns.

Results: The TTP, WI, and SS values of malignant lesions were statistically significant from those of benign lesions ($p < 0.05$). However, the difference for the MRE values was not statistically significant. The distribution of TIC patterns was a helpful indicator of benign or malignant state, however the difference between the two states was not significant.

Conclusion: Dynamic perfusion MR imaging is a helpful tool in differentiating benign and malignant musculoskeletal lesions.

Index words : Magnetic resonance (MR)

Bone neoplasms

Soft tissue neoplasms

Musculoskeletal diseases

Address reprint requests to : Sang Hoon Lee, M.D., Department of Radiology, Asan Medical Center, University of Ulsan College of Medicine,
388-1 Poongnap-dong, Songpa-gu, Seoul 138-736, Korea.
Tel. 82-2-3010-4400 Fax. 82-2-476-4719 E-mail: shlee@amc.seoul.kr, medlsh@stanford.edu